Long-Term Seasonal Trends in Sources and Pathways of Trans-Atlantic Dust Plumes and their Implications for Transport of Microorganisms

Ali Hossein Mardi[1], Miguel Ricardo A. Hilario[2], Regina Hanlon[3], Cristina Gonzalez-Martin[4], David Schmale[3], Armin Sorooshian[2,5], Hosein Foroutan[1,*]

1. Department of Civil and Environmental Engineering, Virginia Tech, Blacksburg, Virginia, USA
2. Department of Hydrology and Atmospheric Sciences, University of Arizona, Tucson, Arizona, USA
3. School of Plant and Environmental Sciences, Virginia Tech, Blacksburg, Virginia, USA
4. Instituto Universitario de Enfermedades Tropicales y Salud Pública de Canarias, Universidad de La Laguna, San Cristóbal de La Laguna, Spain
5. Department of Chemical and Environmental Engineering, University of Arizona, Tucson, Arizona, USA

*Corresponding author: Hosein Foroutan (hosein@vt.edu)

Keywords: Saharan dust, Long-range transport, Trajectories, Microbes, Aerobiology

Key Points:

- Trans-Atlantic dust plumes affect the southeast United States and the Caribbean basin mainly in summer and the Amazon mainly in winter.
- Shorter travel time, higher humidity, and lower UV radiation provide higher chance of survival for microorganisms transported to Amazon.
- Majority of summer dust plumes originate from the western arid regions of North Africa, while winter dust plumes vary in their origin.

Abstract

New information is needed about the potential sources and pathways of trans-Atlantic dust plumes. Such knowledge has important implications for the long-distance transport and survivability of microorganisms. Forward trajectories of trans-Atlantic dust plumes were studied over a 14-year period, between 2008 and 2021 (n =>500,000 trajectories). Two major dust transport patterns emerged from these analyses. First, summer trajectories (June – August) that arrive in the southeastern regions of the United States and the Caribbean basin and travel above the marine boundary layer at an average altitude of 1,600 m. Second, winter trajectories (December – February) that arrive in the Amazon basin and travel within the boundary layer at an average altitude of 660 m. Ambient meteorological conditions such as solar radiation and relative humidity along dust trajectories suggest a more suitable condition for the survivability of microorganisms reaching the Amazon during the winter with a lower mean solar radiation flux of 294 W m^{-2} and mean relative humidity levels at around 61% as compared to averages of 370 W m^{-2} solar radiation and 45% relative humidity for summer trajectories intruding the Caribbean basin. Nevertheless, 14% of winter trajectories (4,664 out of 32,352) reaching the Amazon basin face intense precipitation of higher than 30 mm and get potentially removed as compared to 8% of trajectories (2,540 out of 31,826) intruding the Caribbean basin during the summer. Collectively, our results have important implications for the survivability of microorganisms in trans-Atlantic dust plumes and their potential for major incursion events at receptor regions.

Plain Language Summary:

Each year, dust aerosols from arid northern Africa travel across the Atlantic, impacting areas as far as the Americas. One of the lesser studied aspects of this Trans-Atlantic dust transport is the transport of microorganisms onboard the dust aerosols. We defined two dust receptor subdomains on the western side of the Atlantic Ocean and analyzed the seasonal transport of dust to each subdomain from 2008 to 2021. For trajectories connecting the dust sources to each receptor region, travel path, altitude, and ambient meteorological conditions along the trajectories were studied. During the summer transport season, the majority of aerosols intrude the southeastern regions of the United States and the Caribbean basin. They travel with an average altitude above the marine boundary layer. During the winter transport season, the Amazon basin emerges as the main receptor region of dust trajectories. These trajectories travel at considerably lower altitudes and mainly within the boundary layer. Ambient meteorological conditions such as

solar radiation dose, relative humidity, and travel time suggest a more suitable condition for the survivability of microorganisms reaching the Amazon during winter. However, a greater portion of trajectories face intense precipitation and get potentially removed during that time.

1. Introduction

The most abundant type of aerosol in the atmosphere by mass is dust (Kok et al., 2021a; Kinne et al., 2006) of which the greatest portion is emitted from the surface of desertified regions where evaporation exceeds the mean annual precipitation (Shao, 2008; Kok et al., 2021b). Deserts of North Africa, including the Sahara and Sahel regions are one of the world's most prominent dust sources (Schütz, 1980; d'Almeida, 1986) with the greatest emission contributed by the Sahel area (Ginoux et al., 2012). Dust emissions are not homogeneous over North Africa and some areas are known to have higher emission rates. As an example, the Bodélé depression in Chad is known to be the greatest source of dust emission in the World (Prospero et al., 2002; Washington et al., 2003; Engelstaedter and Washington, 2006) and the western side of North Africa, on the border of Mali and Mauritania is known as another major source of aeolian dust (Engelstaedter and Washington, 2006). Extensive emissions of North African dust contribute to one of the greatest global atmospheric dust transport pathways across the Atlantic (Kellogg and Griffin, 2006), which is sometimes referred to as a dust river (Chakraborty et al., 2021).

After being emitted, North African dust aerosols remain airborne for days until they reach multiple receptor regions located as far as the Amazon, the Caribbean, and the southeast U.S. depending on the season (Prospero, 1999; Prospero et al., 2014). Dust aerosols have the potential to impact the atmospheric microbiome of the receptor regions (Gat et al., 2017; Mazar et al., 2016; Rahav et al., 2016), which can include transport of high-threat or invasive pathogens, depending on the source of emission (Shinn et al., 2003; Griffin et al., 2001; Hara and Zhang, 2012; Favet et al., 2013). Source location can also influence the size distribution of emitted dust particles, travel time, and atmospheric conditions experienced by dust aerosols (Gläser et al., 2015; Grini et al., 2005). This motivates the need for the analysis of dust source locations. Nevertheless, it is challenging to identify the exact source of emission for each receptor region based on current remote sensing or in-situ methods (Engelstaedter et al., 2006; Gläser et al., 2015). Moreover, as dust particles passively travel via global circulation, the amount of transported dust, the regions they reach, and the conditions they experience along the way are driven mainly by prevailing circulation regimes from the emission point to the receptor region (Schepanski et al., 2017). Occasionally, receptor regions such as the Caribbean, Southeast U.S., and Amazon have

experienced anomalous levels of dust due to irregularities in the circulation regime (Yu et al., 2021).

The atmosphere is teeming with microscopic life (Burrows et al., 2009a; Burrows et al., 2009b). Microorganisms thrive in a variety of aquatic and terrestrial environments and knowledge of their sources and potential contribution to the global climate budget has received considerable attention (Jaenicke, 2005, Mayol et al., 2017; Shi et al., 2022). Notes of airborne transport of microorganisms are dated back to early days of discovering microorganisms (Gregory, 1971; Gorbushina et al., 2007). Several cases of modern crop plant diseases are documented to be transported across the continents via aerial dispersion of spores of plant pathogenic fungi (Brown and Hovmøller, 2002). Microorganisms may be transported as individual cells (e.g. spores) (Gregory, 1961), in clusters (e.g., conidiophores), and/or attached to dust particles (Kellogg, 2006). Previous studies of atmospheric dust have revealed the presence of diverse bacterial communities (Giongo et al., 2015; Gonzalez-Martin et al., 2014; Favet et al., 2013; Yamaguchi et al., 2012). Traces of atmospheric dust have been found in the most remote areas of the world with estimated travel time-scales at around 13 days (Iwasaka, et al., 1983; Uno et al., 2009; Zhang et al., 2007). Consequently, microorganisms traveling with dust have the potential to be transported around the world.

Though trans-Atlantic transport of dust has been the subject of a considerable amount of research (Gläser et al., 2015, and references therein), the long-range co-transport of microorganisms and dust aerosols is one of the lesser studied aspects of this phenomenon (Schuerger et al., 2018). New information is needed about the atmospheric trajectories of trans-Atlantic dust, sources contributing to them, and their implication for microorganisms' transport. In this manuscript, we examined seasonal trends in atmospheric trajectories of trans-Atlantic dust over a period of 14 years (2008-2021). We hypothesize that seasonal trends observed in dust emission sources, travel path, and ambient meteorological conditions along these trajectories will lead to distinct environmental conditions that can benefit the co-transport of different taxa of microorganisms, depending on the season and the receptor region. To test this hypothesis, we combined a dust emission scheme and forward trajectory analysis to characterize ambient conditions along each dust transport trajectory from the point of emission until it reached our defined receptor regions. The specific objectives of this study were to (1) connect dust source and receptor regions across the Atlantic Ocean, (2) report on the seasonal trends observed in dust trajectories and ambient

conditions along the way, and (3) explore possible implications related to concentration, diversity, and longevity of the co-transported microorganisms.

After locating major seasonal sources of dust, we report defined initiated from North African sources that reach two receptor regions located on the western side of the Atlantic Ocean (US-CARIB and AMZN). We report on the spatial and vertical distribution of these trajectories through different seasons to depict a seasonally resolved demonstration of dust travel across the Atlantic. Next, we discuss the amount of dust emission associated with these trajectories to isolate emission areas with relative importance for defined receptor regions. In the final section, we discuss the average meteorological condition experienced by the majority of the dust trajectories across the Atlantic and its potential influence on the type, concentration, and diversity of co-transported microorganisms.

2. Data and Method

2.1. Dust Emission Sources

NASA Modern-Era Retrospective analysis for Research and Applications, Version 2 (MERRA-2; Gelaro et al., 2017) is a continuation of the modern satellite era (1980 onward) atmospheric reanalysis run and managed by the NASA Global Modeling and Assimilation Office (GMAO). The MERRA-2 system incorporates more contemporary datasets not available to the original MERRA reanalysis dataset with an improved meteorological observing system. One of the greatest advantages of MERRA-2 is having analyzed aerosol fields that can be used as an input in analysis of the interaction between aerosols and regional climate.

In MERRA-2, dust mass mixing ratios are simulated with a radiatively coupled version of the Goddard Chemistry, Aerosol, Radiation, and Transport model (GOCART) for five non-interacting size bins. Dust emission is derived based on a map of potential dust source locations, according to the observed co-location of large-scale topographic depressions and dust emitting regions. Dust emission values are wind driven for each size bin and calculated based on the parameterization provided by Marticorena and Bergametti (1995). Even though the MERRA-2 reanalysis model incorporates the deposition and hygroscopic growth of the aerosols after their emission, in this study we use the MERRA-2 dust emission scheme only to isolate the emission hotspots based on their long-term seasonal activity.

MERRA-2 hourly dust emission data were obtained for 2008-2021 (collection M2T1NXADG, DOI:10.5067/HM00OHQBHKTP), in five different size bins (DUEM001-005, kg m^{-2} s^{-1}) covering a dry size range from 0.1-10.0 µm for an area in North Africa covering 12°N - 38°N and 18°W - 40°E (Figure 1). Hourly emissions of different size bins were summed up for each day to create daily dust emission value maps with a spatial resolution of 0.5° × 0.625°. To obtain the seasonal dust emission hotspots, first the daily emissions of all days of that season were averaged to create a composite map of average seasonal emission. Next, a Gamma distribution was fitted to the pixel values of each map and the 80th percentile on the corresponding cumulative distribution function was selected as the threshold. On each map, the pixels with seasonal average values greater than the threshold obtained for that season were nominated as the seasonal dust emission hotspots. Finally, for each pixel of the nominated dust emission hotspots and during each day of that season, if the daily dust emission value was greater than 85th percentile of total daily emission values, that day was selected as a significant dust emission day for that pixel. Hereafter, we refer to these incidents as dust emission activities. Both 80th and 85th percentile thresholds were tuned to cover the majority of seasonal dust emission areas and be inclusive of the majority of daily dust emission incidents yet, keep the total number of trajectories within our data processing capacities. Over the course of study, more than 500,000 pixels of dust emission activities were nominated by this method and provided as inputs to the trajectory analysis.

2.2. Dust Atmospheric Pathways

To track the dust emission activities and report on their endured condition along the trajectories, NOAA Hybrid Single-Particle Lagrangian Integrated Trajectory model (HYSPLIT) was used (Draxler and Rolph, 2010; Rolph et al., 2017; Stein et al., 2015). For each pixel designated as a dust emission activity, trajectories were initiated in forward mode from an altitude of 300 m above the ground level on a daily basis. This altitude was selected to minimize the risk of trajectories interfering with surface terrain. All of the trajectories were initiated at 00:00:00 UTC and run for 360 hours, equivalent to 15 days to assure that the majority of the trajectories reached the downwind receptor regions. Two receptor regions were defined in the downwind area (Figure 1), one covering the southeast U.S. and Caribbean (5°N - 25°N and 65°W - 95°W, US-CARIB from now on) and the other covering parts of the Amazon (10°S - 5°N and 50°W - 85°W, AMZN from now on). The location and boundaries of the receptor region were defined based on the reported oscillation pattern of trans-Atlantic dust transport trajectories due to the seasonal variation of the inter tropical convergence zone (ITCZ) over the Atlantic Ocean (Doherty et al., 2012; Gläser et al., 2015). Locations were selected to ensure they receive the majority of westward trajectories

originating from the North African arid areas. The NCEP/NCAR Reanalysis archived data were used for HYSPLIT runs, and meteorological data were reported along the trajectories. The top of the model was set at 10 km, and the meteorological data file directly handled the vertical motion in the model.

Forward trajectory analysis is prone to a series of errors, including but not limited to the coarse resolution of the meteorology files and long trajectory run time (Stein et al., 2015; Wotawa and Kalinowski, 2000; Dadashazar et al., 2021; Hilario et al., 2021 and references therein). Additionally, the embedded uncertainties in the dust emission scheme do not enable us to report on properties and fate of each individual dust emission trajectory with certainty. However, by combining more than 500,000 trajectories over a period of 14 years, our analyses are expected to yield notable results and gauge the uncertainty associated with the trajectory model (Harris et al., 2005) for the seasonal trends governing the majority of dust trajectories connecting North African sources to Middle West Atlantic Ocean receptor regions.

Of all dust trajectories sourced from North Africa, only westward trajectories that reach either one of receptor regions were isolated for further analysis. It is possible for a trajectory to impact more than one region and be counted for both. For a trajectory to impact a receptor region, the average altitude of trajectory inside that region must be below 5 km. This criterion was defined to neglect those trajectories that pass above the receptor regions at higher altitudes. The general direction of each trajectory was calculated by adding up the trajectory longitude for one third of the total number of steps for each trajectory and trajectories moving east of their emission points were neglected. This was done to avoid trajectories that reach westward receptor regions by circling the globe in eastward direction, even though we do not expect to encounter a great number of such trajectories.

2.3. Meteorological Parameters

For each forward trajectory, the mean downward solar radiation flux (W m^{-2}), ambient temperature (K), relative humidity (RH, %), and precipitation (mm hr^{-1}) from NCEP/NCAR Reanalysis were calculated for the duration of travel time from the emission point to the receptor region. In addition to the means, values were also integrated for the travel path to reflect the total impact perceived by each trajectory and account for differences in travel times. By multiplying the solar radiation flux by number of steps with an hour of duration for each step, total solar radiation dose (J m^{-2})

was calculated for each trajectory, similar to the methodology used by Kowalski (2010). For ambient temperature and RH, we used an integration scheme as follows:

$$T_{amb,P} = \left(\sum_{i=1}^{n} \frac{1}{T_{amb,i}}\right) \times n \quad (1)$$

In equation (1), $T_{amb,P}$ is the path integrated value of $1/T_{amb}$ over n number of steps for each trajectory with the unit of hr.K^{-1}. The purpose behind integrating the inverted values of T_{amb} is to reach a higher integrated value for trajectories experiencing lower temperature for a longer time. Similarly, $RH_{amb,P}$ is calculated for the duration of each trajectory with a unit of hr.percent^{-1} RH and a higher number reflects a lower RH impacting the aerosols for a longer period of time.

3. Results and Discussion

3.1. Forward Trajectory Analysis

Table 1 summarizes the number of trajectories reaching each receptor region during each season. From more than 500,000 dust associated trajectories emitted from the North Africa, 115,715 trajectories (23%) impacted either one of designated receptor regions. Each one of the receptor regions has received approximately half of the total trajectories with 68,564 and 56,113 trajectories reaching US-CARIB and AMZN, respectively. Together, these numbers add up to 124,677 trajectories which include 8962 trajectories that have impacted both sub-domains and were accounted for both. Selection of receptor regions, based on the seasonal oscillation of the cross Atlantic dust transport pathway can be the reason behind receiving approximately half of trajectories at each region. This oscillation is likely due to the seasonal change of the latitudinal location of the ITCZ (Gläser et al., 2015).

The majority of the trajectories reached US-CARIB during June-August with an average latitude of 17.5°N, and AMZN during December-February with an average latitude of 9.6°N, which is also evident in Figure 2 (panels a-h). Results obtained for both the seasonality and the transport pathways are consistent with previous reports on trans-Atlantic dust transport (Schepanski et al., 2009; Chiapello et al., 2005; Gläser et al., 2015, and references therein). Another notable difference among the receptor regions was the altitude at which the trajectories traveled before reaching each receptor region. As depicted in Figure 2 (panels i-p), the summer trajectories

reached higher levels of the free troposphere immediately after they leave the African continent at about 25°W with an average altitude of 1,639 m for US-CARIB trajectories during the June-August season. In contrast, the winter trajectories reaching the AMZN traveled over a notably lower mean altitude of 663 m from December to February. The different seasonal trajectory path and altitude have implications for longevity, concentration, and diversity of onboard microorganisms as it implies different mean temperatures, solar radiation dose, and RH are experienced by microorganisms (Chen et al., 2020; Kowalski and Pastuszka, 2018). More details of trajectories' seasonal mean path and altitude can be found in Table S1.

Figure 3 shows the seasonal histograms of travel duration for trajectories impacting each receptor region. On the histograms, a cut off is evident at 360 hours which is due to 360 steps duration chosen for forward trajectories. The existing limitation in the number of steps does not allow for a complete depiction of dust trajectories. Nevertheless, we believe that the selected number of steps allows capturing of the majority of dust trajectories that reach the receptor regions because the travel time at which the highest number of trajectories travel are captured with the current run time. We do not expect to see a new peak for travel times higher than fifteen days because the longest travel times mentioned for African dust carrying trajectories are in the orders of fifteen days (Gläser et al., 2015) and this was the basis for selecting the current number of steps. It should also be noted that trajectories with longer travel times have lower possibility for transporting viable cultures of microorganisms, due to having microorganisms exposed for a longer period of time to the atmospheric extreme environment (Smith et al., 2011).

Comparing peak seasons of December – February and June – August, summer time trajectories spend a longer period of time traveling before reaching the receptor regions, which implies a lower possibility for transporting viable microorganisms due to being exposed to harsh atmospheric environment for a longer period of time. Trajectories reaching AMZN from December – February have a more uniform distribution with peak number of trajectories taking between 200 to 250 hours to travel (Figure 3-a); however, the number of trajectories taking longer than 250 hours is also notable. On the other hand, trajectories reaching US-CARIB from June to August show a skewed distribution with peak number of trajectories occurring between 240 and 280 hours (Figure 3-c). The average travel time of trajectories is also summarized in Table S2. Comparing the two peak seasons, the total number of trajectories taking less than 200 hours to travel is considerably higher during the AMZN peak season (10468 versus 3997, Figure 3-a), which implies a higher probability of survival for the co-transported microorganisms. Additionally, the

two datasets were analyzed via a Student's t-test for the difference of the means and results indicate that summertime trajectories impacting the US-CARIB travel on average for a significantly longer period of time compared to wintertime AMZN trajectories with higher than 95% statistical confidence.

Shorter travel times for AMZN peak season trajectories can be partly attributed to the shorter distance between the Amazon and arid regions of northern African continent (Gläser et al., 2015). Additionally, long-term variations in the large-scale circulation regime over the tropical north Atlantic can cause irregularities in the transport of dust aerosols across the Atlantic. Examples of such interactions would be the impact from wide spread deforestation over tropics on increased dust transportation via weakening of the Hadley cell (Li et al., 2021) or connection between the seasonal amount of rainfall in the Sahel region and the amount of seasonally emitted dust (Brooks and Legrand, 2000).

From December to February, trajectories reaching the US-CARIB travel at time scales similar to the AMZN trajectories while the mean travel time from June to August is higher for trajectories reaching the AMZN. Relatively longer mean travel time of the summer trajectories impacting the AMZN sub-domain can be explained by differences observed in the transport regime of such trajectories. In a relevant study and over an 8 years period of 1995 – 2002, during July – October, Dunion (2011) reports an average wind velocity of 5 m s^{-1} for trajectories described as moist and tropical with characteristics similar to those impacting the AMZN sub-domain. In the same study, trajectories described as Saharan air layer travel considerably faster, with an average wind velocity of 9 m s^{-1}. From March to May, the observed pattern for travel times is somewhat similar to June – August. However, outside the peak seasons the number of trajectories is considerably lower. From September to November, trajectories of both receptor regions demonstrate similar travel times with a higher number of trajectories reaching US-CARIB.

3.2. Dust Emission Activities

To isolate North African dust (and potential microorganisms) sources contributing to each receptor region, composite maps of dust emission activities were made by summing up total seasonal dust emission activity associated with trajectories impacting each receptor region (Figure 4). By focusing only on emissions capable of reaching our receptor regions on the western coasts of the Atlantic, the new seasonal maps differ from the mean seasonal dust emission maps (compare Figure 4 and Figure S1). These new sets of maps are made for 124,677 trajectories that have

impacted either one of receptor sub-domains including 8,962 trajectories that are counted for both. On the maps, most emission regions were clustered around the west and southern regions of the North African continent with minimal impact from the north and eastern sources, even though on seasonal analysis, north and eastern regions demonstrated statistically significant dust emission levels based on a Gamma distribution fitted to the long-term daily emission values of each pixel. Such composite maps of seasonal dust emissions are also presented in Brooks and Legrand (2000) study of dust variability over Northern Africa with spatial patterns following Figure 4, even though timespans selected as seasons are slightly different from this study.

For the US-CARIB region, the June to August emissions stand out from the other seasons. This would be no surprise as it is also the season during which the majority of trajectories reach this receptor region. Similarly, during the December-February season when the majority of trajectories reach AMZN, total dust emission associated with these trajectories is most distinct, compared to the rest of the year (Figure 4-b). Comparing the June - August season of US-CARIB with December - February season for AMZN enables us to better understand which North African sources have the highest impact on each receptor region. For the US-CARIB region and during the high dust season (June - August), the majority of emissions come from sources located on the western half of North Africa. This follows the results reported by Gläser et al., (2015), even though the extent of the receptor regions slightly differs between the two studies. Winter was observed as the peak season for dust transport to AMZN with a great impact perceived from Bodélé depression emissions, in accordance with previous studies (Bristow et al., 2010; Washington, et al., 2009).

Focusing solely on the long-term seasonal averages or total emission maps might obscure the interannual variations in the location of dust sources impacting each receptor region the most. For this reason, we had a closer look at the interannual variations in the equivalent center of dust emission for each receptor region. The latitude and longitude for the equivalent dust emission center is calculated based on the following formulas:

$$Lat = \frac{\sum_{i=1}^{n} E_i Lat_i}{\sum_{i=1}^{n} E_i} \quad (2a)$$

$$Lon = \frac{\sum_{i=1}^{n} E_i Lon_i}{\sum_{i=1}^{n} E_i} \quad (2b)$$

In equations (2a,b), n represents the number of dust-emitting pixels on each panel of total seasonal dust emission maps for a certain year, E_i represents the emission associated with a certain pixel, and Lat_i and Lon_i are the latitude and longitude of that pixel, respectively. The seasonal location of the equivalent dust emission centers for trajectories impacting each receptor region are shown in Figure 5. Except for trajectories reaching US-CARIB in the peak season of June - August, the location for the center of emission experienced notable spatial variation throughout the years, moving along a diagonal line between south-central and north-western parts of North African desertified regions. Almost all of the interannual spatial variation in the center of emissions happens along this line, connecting the western emission sources and the Bodélé depression, which denotes the profound role of these two regions in driving the equivalent dust emission source. The strong impact from these two regions is also frequently mentioned in the literature but to the best of our knowledge, no previous study has looked at the longer interannual trend. As an example, Wagner et al., (2016) compared the emission source between 2007 and 2008 and mentioned 2008 as the year with the greatest impact from the Bodélé depression. We do not have the data from 2007 but our results demonstrate the heaviest impact from Bodélé in 2008, from December to February. In a similar study, Barkley et al., (2022) studied the North African dust emissions during 2014 and 2016 and captured the heavy dust emission activity from Bodélé that dragged the center of emission towards the south-central region. Similarly, in our results, the dust emission center is shifted toward the central regions in 2016, which denotes a higher impact from Bodélé in that year. Long term variations in the equivalent center of dust emissions can also be impacted by ongoing variations in greater scale meteorology over the tropical Atlantic Ocean. In a related study, Li et al (2021) analyze the long-term impact of deforestation in tropics on African dust emissions and reports a shift in the location of peak surface dust concentrations toward the south as a result of a change in the albedo of tropics, induced by deforestation. This interconnectedness of dust emissions to the greater variations in the governing circulations regimes over the Atlantic Ocean motivates future studies in this field, beyond the scope of the current study.

Another intriguing finding in the study period is the small variation observed in the equivalent dust emission source location for trajectories reaching US-CARIB during the peak of June to August, in contrast to the variation observed for AMZN during its peak of December to February. Considering the ongoing debate about the role of the Bodélé depression in trans-Atlantic dust transport, perhaps dividing the receptor region into smaller sub-domains could result in a more detailed and resolved answer about the origin of dust aerosols impacting the Western Central

Atlantic Ocean receptor regions. Current results indicate that when combined with trajectory analysis, emissions from the Bodélé depression do not have as profound of an impact on the US-CARIB region as compared to AMZN. Additionally, it should be noted that based on these results, even though Bodélé plays an integral role in dust emissions impacting the AMZN, it is not the sole source contributing to the annual dust load. These results are notable as distinct geographical regions will emit distinct taxa of microorganisms (Favet et al., 2013); hence, based solely on the origin of emissions, higher interannual diversity is expected for emissions impacting the AMZN receptor region.

3.3. Ambient Meteorological Conditions Along the Trajectories

The diversity and concentration of viable microorganisms arriving at each receptor region is linked to the amount of dust traveled as well as the meteorological parameters along the trajectory (Prospero et al., 2005). The erythemal part of the solar ultraviolet (UV) radiation, which mainly consists of UV-B (280–315 nm) is one of the main factors reducing the viability of microorganisms from the upper atmosphere, especially ones with lower resistance to UV radiation (Yang et al., 2008). Desiccation and extreme temperatures in the upper levels of troposphere may also reduce the viability of microorganisms during transit (Griffin et al., 2007). Consequently, we examined the mean solar radiation flux, ambient temperature, and RH along the trajectories in an effort to highlight the differences observed in meteorological conditions of different seasons and discuss the potential impact they have on the viability of microorganisms during transport from emission sources to receptor regions. Additionally, we analyzed the accumulated amount of precipitation perceived by each trajectory, as a measure of dust aerosol removal due to wet deposition.

Figure 6 compares the histograms of average solar radiation flux, ambient temperature, and RH along the trajectories for dust aerosols reaching US-CARIB during the June – August, and AMZN during the December - February season. Only the peak seasons with the highest number of trajectories were compared to demonstrate the contrast between the two peak dust transfer seasons. Regardless of the region, trajectories receive higher and more uniform levels of mean solar radiation during the June to August season with an average of 370 W m^{-2} for the US-CARIB region as compared to 294 W m^{-2} for the AMZN region (Figure 6-a and b). Additionally, the spatial distribution of trajectories colored with average received solar radiation flux is depicted in Figure 7 (panel a and b) for the same seasons. The area denoted with contours of 1, 5, and 10 on each panel of Figure 7 denotes the pixels with 1, 5, and 10 percent of total seasonal dust emissions passing above them, respectively. In other words, the majority of total seasonal dust emission passes through the denoted corridors. For the AMZN, the average received solar radiation flux is

higher for those trajectories passing from lower latitudes yet trajectories reaching the US-CARIB region demonstrate a more uniform distribution, latitudinally.

Relying solely on average values would be an oversimplification of the impact from meteorological parameters, and the cumulative amount of time a trajectory receives a certain level of solar radiation is another key parameter impacting the longevity of microorganisms. Panels (a) and (b) in Figure 8 demonstrate the histograms of the cumulated solar radiation fluxes in form of the solar dose by summing up hourly averages. Considering the duration of travel time, histograms are now more dispersed and trajectories are impacted by a wider range of solar dose. Still, solar doses are higher on average for both receptor regions during the June to August peak season and trajectories demonstrate a more distinct peak.

The erythemal UV portion of the total atmospheric irradiance is dependent on geographic location, time of the year, and total ozone column concentration in the atmosphere and is discussed in detail by Utrillas et al. (2018). Following their results, we assume 0.02% of total atmospheric irradiance as erythemal UV radiation. Using this conversion rate, dust trajectories are estimated to be exposed to UV radiation levels ranging from 20 – 100 KJ m^{-2}. To provide some context, it is reported that UV radiation levels of around 40 J m^{-2} are capable of a one log decrease in concentration of microorganisms in a single stage decay model (Kowalski, 2010), which decreases the chance of survival for non-UV resistant microorganisms to extremely low levels. However, certain UV resisting strains of microorganisms are capable of surviving up to 2 KJ m^{-2} of UV radiation with minimal decay and no negative correlation with UV concentration, which increases their chance of survival in extreme atmospheric conditions (Yang et al., 2008). The established positive increase in the concentration of viable microorganisms from samples of long-range transported dust is suggestive of co-transported microorganisms' capability to survive the extreme atmospheric environment, within dense dust plumes (Schlesinger et al., 2006) and in spite of extremely high doses of erythemal UV radiation. Survival microorganisms during extreme atmospheric conditions can be partly explained by attenuation of UV radiation by dust aerosols at higher levels of atmosphere (Herman et al., 1999) or microorganisms being shielded from UV radiation within the cracks and crevasses of inorganic dust aerosols (Griffin et al., 2001). Furthermore, adapting UV resistant abilities such as forming cell clumps or aggregates can increase microorganisms' UV survivability (Yang et al., 2008), which is a common feature among microorganism taxa that are usually found in desert soils (Musilova et al., 2015). It is hypothesized that similar DNA repair characteristics, which make a phenotype resistant to UV radiation, will

also increase the ability to survive other environmental stressors such as desiccation (Rainey et al., 2005), and therefore, UV resistance can be considered the key parameter in survivability of microbes in the atmosphere.

Next, we compared the average ambient temperature along the trajectories for the same seasons and regions. No discernible difference can be noted between the regions with an average of 293.5 K for US-CARIB from June to August as compared to 294.1 K for AMZN from December to February. Moving from the most southern latitudes of this corridor up to the highest ones, a difference of around 5 K is noted for the trajectories during the both seasons but in the middle of the corridor where the trajectories are more concentrated, average ambient temperature is the highest and most uniform.

Compared to histograms of average conditions, histograms of path-integrated ambient temperatures (see Eqn. (1)) are more dispersed, mainly due to variable travel time of trajectories (Figure 8, panel c and d). The peak value appears around 150 – 250 hr K^{-1} for trajectories reaching US-CARIB from July to August and from 50 – 150 hr K^{-1} for AMZN trajectories from December to February. Mean values do not exhibit a significant difference, hence, the observed difference of path-integrated ambient temperature is mainly due to different travel times of trajectories reaching each receptor region. For atmospheric microorganisms, there is evidence in support of high temperature as a suitable condition and low temperature as the limiting factor for the survivability of microorganisms (Almaguer et al., 2014). As lower mean path integrated ambient temperatures represent higher temperatures endured for a longer time (see Eq. 1), transport condition is more suitable for survivability of microorganisms transported to AMZN between December-February. Nevertheless, Zhai et al. (2018) reviewed results from numerous studies of temperature impacts on the survivability of microorganisms in the atmosphere and reported some contradicting results, and thus, concluded that the range of atmospheric conditions and type of microorganisms should be taken into consideration.

Finally, the RH along the trajectories is compared for the peak seasons with an average of 45±11% for trajectories reaching US-CARIB during the June - August season and 61±13% for AMZN during the December – February season. Compared to US-CARIB, the distribution of AMZN trajectories is more skewed with more trajectories experiencing a higher RH (Figure 6-e and f) and a bimodal distribution. It was discussed earlier that majority of the summer-time trajectories travel above the boundary layer, while the majority of winter time trajectories travel at

much lower altitudes and within the marine boundary layer (see panels k and m in Figure 2). As a result, the difference between the averages of RH for the bulk of trajectories in two peak seasons can be attributed to the sharp difference in RH observed above and within the marine boundary layer (Wulfmeyer and Feingold, 2000).

During the December-February season, a striking divergence can be seen in the histograms of RH for trajectories reaching the AMZN region. This is characterized by a bimodal distribution, which is attributed to an increased number of trajectories originating from Bodélé and spending more time traversing arid regions. Among the meteorological parameters examined, RH exhibits the most significant contrast between land and ocean, which is to be expected as the ocean plays a significant role in determining RH levels. This is evident on panel f in Figure 7 and for trajectories sourced from the Bodélé depression that spend a longer time over continental Africa, and hence, experience lower mean levels of RH.

RH also has a crucial role in the removal of aerosols by increasing their size through hygroscopic growth and accelerating the rate of dry deposition (Williams, 1982). This is due to the fact that even a small increase in particle size can significantly boost their fall velocity by up to 10 times, leading to a faster rate of dry deposition (Arimoto et al., 2003). Based on some modeling analysis, this increase can be even higher for particles with a diameter in the range of 0.1 – 10 μm, which include a great portion of dust aerosols (Sengupta et al., 2021). Based on the literature, the RH level of 98% was assumed as a criterion above which the size of particles increases significantly due to hygroscopicity (Williams, 1982, Koehler et al., 2009). Even though aerosol hygroscopic growth can occur at RH levels around 70%, such high levels of RH are selected due to the hydrophobic nature of Saharan dust relative to more hydrophilic aerosols commonly found in the atmosphere (Kaaden et al., 2009). In addition to the dry deposition, wet scavenging of dust aerosols during precipitation periods is another mechanism for their removal from the atmosphere. This motivates the analysis of the cumulative time aerosols spent under the influence of RH levels above 98% and as a function of total accumulated precipitation along the trajectories. For context, Dadashazar et al. (2021) calculated a 53% reduction in the ratio of $PM_{2.5}$ relative to background CO levels when comparing >13.5 mm accumulated precipitation along trajectories from North America to Bermuda versus trajectories with <0.9 mm accumulated precipitation. Hilario et al. (2021) demonstrated that a higher accumulated precipitation along trajectories was associated with much lower aerosol concentrations during transport over the West Pacific. The impact of precipitation along the trajectories was also studied along trajectories originating from

the South American continent and moving toward the Pacific Ocean (Freitag et al., 2014). They concluded that trajectories with accumulated precipitation above 50 mm demonstrate distinctive characteristics of wet scavenging on plumes.

Figure 9 compares histograms of accumulated precipitation along the trajectories impacting each sub-domain during the June – August and December – February seasons. Average accumulated precipitation along the trajectories was 13.69 and 18.16 mm for US-CARIB and AMZN, respectively. Similar to RH, higher mean precipitation values for AMZN trajectories can be accounted for in part by lower mean transport altitude (Figure 2) and hence, a higher chance of being intercepted by precipitating clouds. On the contrary, US-CARIB trajectories travel at higher altitude, which increases their chance of being transported above the precipitating systems. It is worth mentioning that two main mechanisms of convective cold pools and the nocturnal low-level jets account for more than 80% of dust emission incidents over the arid regions of Africa. Both mechanisms meteorologically drive the dust emission over the warm and dry continental North Africa during the summer, where extremely low levels of moisture exist in the atmosphere (Heinold et al., 2013). As dust layer reaches the west African coast, it slides above the cool marine air mass and is lifted to higher altitudes (Van Der Does et al., 2018). All these processes give the trajectories little to no chance of being intercepted by precipitation before leaving the continental regions.

Field measurements also confirmed that there is an increase of up to three times in RH levels within the boundary layer compared to drier conditions in the free troposphere (Maring et al., 2003). Another explanation of higher precipitation along the wintertime trajectories would be the location of high precipitation band across the Atlantic Ocean. Summertime precipitation across the tropical Atlantic Ocean happens between 0° N – 15° N (Siongco et al., 2017) and shifts southward, between 10° S – 10° N during the winter (Barreiro et al., 2002). In both seasons, the greater portion of the precipitations occur in close proximity to the coast of South American Continent. As the majority of summertime trajectories travel above and parallel to the summer band of precipitation (Figure 7), a lower portion of them are intercepted and washed out by heavy precipitation while on the other hand, wintertime trajectories travel within high precipitation zones and hence, endure a higher precipitation along the trajectories.

Around 14% of AMZN trajectories exhibit accumulated precipitation levels higher than 30 mm, compared to around 8% percent of US-CARIB trajectories. We did the same analysis for the

duration each trajectory spends in RH levels above 98% (not shown in figure). Of the trajectories impacting AMZN, around 4.7% spend at least one hour in such conditions. The analogous analysis for US-CARIB trajectories reveals significantly lower values (<0.2%). Overall, the combined impact of ambient moisture levels, either in form of precipitation or high RH levels is not strong enough to totally eliminate the airborne dust from the atmosphere, however, it should be considered in assessing the amount of dust reaching each receptor sub-domain.

3.4. Implications for the Transport of Microorganisms

The effect of meteorological factors on the survival of airborne microorganisms has been widely studied (Tang et al., 2009). Bacteria, virus, and fungi have different characteristics that help them overcome adverse atmospheric conditions (e.g., extreme temperatures, low water and nutrient availability, high solar radiation, desiccation). Cellular characteristics, such as rigid cell walls in gram-positive bacteria, make microorganisms more resistant to damage. Also, spore-forming microorganisms, like fungi and some bacteria, can survive under adverse circumstances, because they are able to stop or decrease their metabolism.

Traditionally in studies of airborne microorganisms, temperature and RH have been considered to have a positive impact on microbial abundance (Mouli et al., 2005; Harrison et al., 2005; Sun et al., 2022). However, this seems to be partially true only for culture-based studies. Next-generation sequencing analyses of airborne communities have not detected such correlation (Bowers et al., 2012; Shin et al., 2015; Núñez et al., 2021; Zhen et al., 2017), and some even have described how bacterial richness may increase under low temperature conditions (González-Martín et al., 2021). Upon closer look, meteorological factors, such as temperature or RH may have specific influence over different groups of microorganisms. For instance, Park et al. (2020) found a negative correlation between temperature and the phylum Proteobacteria, while this correlation was positive with the Firmicutes and Bacteroidetes phyla. Some authors consider that at higher temperatures, the solar radiation usually increases as well, which can lead to a decrease in the microbial survival rates due to DNA damage (Sun et al., 2022).

By considering how the microbial airborne community may change due to factors such as continuous mixing with atmospheric aerosols and deposition during their transport, specific protective mechanisms unique to each microbe, and specific characteristics of each dust event (e.g., particle sizes, dust plume altitude, and amount of dust), the effects of the environmental factors and chance of survival may be predicted for specific groups of microorganisms.

4. Conclusions

In this study, we integrated the NASA MERRA-2 dust emission scheme with the NOAA HYSPLIT forward trajectory analysis to study spatiotemporal characteristics of more than half a million trajectories carrying dust aerosols across the Atlantic during a 14-year period (2008-2021). We followed the dust transport pathway from its emission sources over Sahara and Sahel regions in North Africa until reaching receptor areas as far as the southeast U.S., Caribbean, and Amazon. Along the transport paths, we studied the meteorological conditions endured by dust aerosols with main focus on parameters impacting concentration, diversity, and longevity of co-transported microorganisms. Results are suggestive of the following conclusions:

- The majority of westward, dust-carrying trajectories enter the southeastern regions of the United States and the Caribbean basin during the summer season (June – August). In winter (December – February), the majority of trajectories enter the Amazon basin. Other seasons of the year serve as transitory times when the total number of westward trajectories are split between the two sub-domains.

- Vertical structure of travel paths is significantly different between the two seasons. During summer (June – August), trajectories traverse the Atlantic at a significantly higher altitude compared to winter (December – February) trajectories. Summer trajectories mainly travel above the marine boundary layer and demonstrate characteristics reported by previous studies on the Saharan air layer (Karyampudi and Carlson, 1988; Tsamalis et al., 2013; Dunion and Marron, 2008). In contrast, winter trajectories spend a greater portion of their travel time within the marine boundary layer in a relatively cooler and moist ambient environment.

- Analysis of dust emission incidents associated with trajectories suggests that during the summer time, the majority of dust intruding the US-CARIB basin is emitted from sources located on the western side of arid regions of northern Africa. However, other source regions such as the Bodélé depression play a role as well. During the winter time and for trajectories impacting the AMZN sub-domain, the Bodélé depression emits the greater portion of the intruding dust but source regions are not clustered as clearly as they are during the summer. Distinct emission sources during each peak season suggest different taxa of microorganisms

being co-transported with dust aerosols. Additionally, a higher diversity of microorganisms is expected during the winter due to a more diverse source base.

- Long-term analysis of dust emitting regions during the peak seasons suggests an interannual oscillation in the equivalent center of emissions for the winter time between the western regions and the Bodélé depression. However, during summer, such spatial variation is not as profound and emission sources are more clustered. Accordingly, a higher interannual variation is expected for the taxa of microorganisms being co-transported with dust aerosols during the winter.

- During summer, trajectories endure significantly higher and more uniform levels of solar UV radiation when compared to the winter season. Endured RH is also lower on average for the summer time trajectories intruding the US-CARIB sub-domain. A bimodal distribution is observed in the histogram of the mean RH endured by wintertime trajectories impacting the AMZN sub-domain. Overall, ambient meteorological conditions are less suitable for the survivability of co-transported microorganisms during summertime.

- Periods of intense precipitation and high RH contribute to the removal of dust aerosols from the atmosphere, however, the total number of trajectories impacted by such conditions constitute no more than 14% of trajectories reaching AMZN sub-domain in winter and 8% trajectories reaching the US-CARIB sub-domain in summer. These transport conditions promote a more suitable environment for long-range transport of microorganisms.

The present study is a part of the ongoing NASA Microbes in Trans-Atlantic Dust (MITAD) field campaign, which aims to investigate microbial long-range transport and survival in dust plumes via an interdisciplinary approach that integrates multiplatform observations such as remote sensing, reanalysis, and atmospheric simulation data with microbiological analysis performed on a series of dust samples, collected at multiple locations across the Atlantic Ocean. Future studies will focus on specific taxa of airborne microorganisms detected in actual dust samples and the correlation between their concentration, diversity, and longevity and environmental conditions in the atmosphere.

Data Availability Statement

MERRA-2 dataset used in preparation of this manuscript can be accessed from (https://doi.org/10.5067/HM00OHQBHKTP) and NCEP/NCAR meteorology files used for HYSPLIT trajectory analysis are stored in (ftp://ftp.arl.noaa.gov/pub/archives/reanalysis).

Acknowledgement

This research is supported by the National Aeronautics and Space Administration (NASA) under Grant 80NSSC20K1532. AS and MRAH were supported by NASA Grant 80NSSC19K0442 for ACTIVATE, a NASA Earth Venture Suborbital-3 (EVS-3) investigation funded by NASA's Earth Science Division and managed through the Earth System Science Pathfinder Program Office. The authors acknowledge the NOAA Air Resources Laboratory (ARL) for the provision of the HYSPLIT transport and dispersion model and READY website (http://ready.arl.noaa.gov) used in this work.

Tables

Table 1 - The seasonal change in the number of trajectories that occurred during each defined seasonal range for the two sub-domains, the southeast United States and Caribbean (US-CARIB) and Amazon (AMZN).

# Trajectories	Dec. - Feb.	Mar. - May	Jun. - Aug.	Sept. - Nov.	Total
US-CARIB	7839	9377	31826	19522	68564
AMZN	32352	11883	3305	8573	56113
Total	40190	21260	35131	28095	124677

Figures

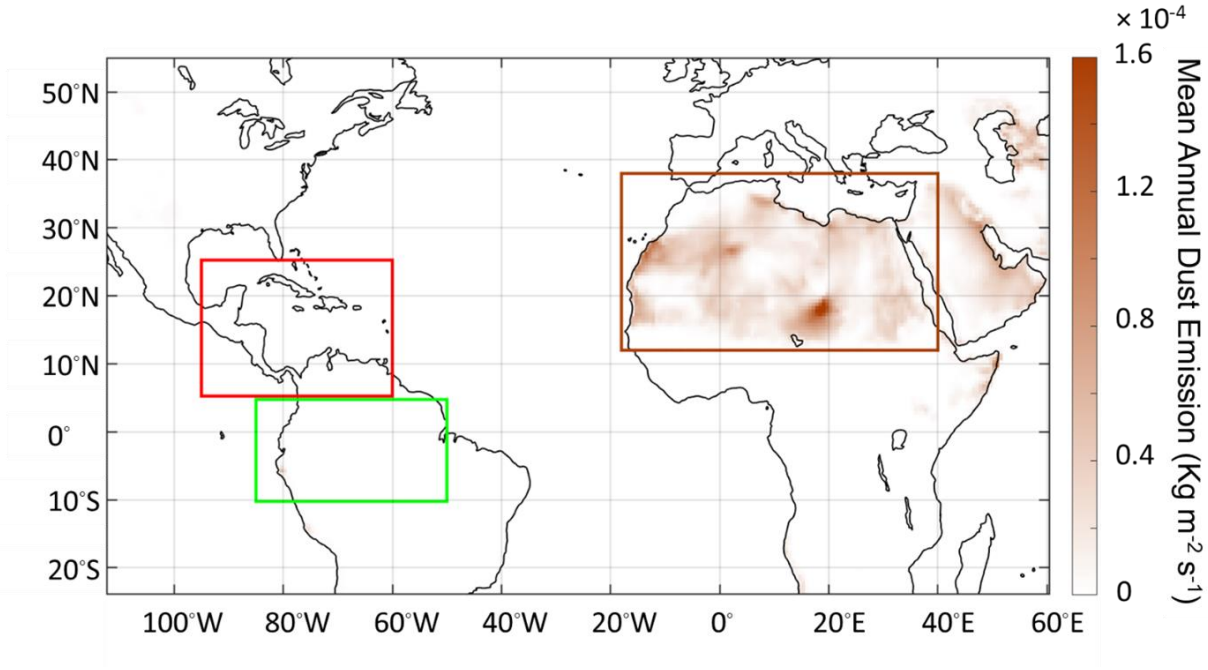

Figure 1. The approximate boundaries of the study region. Two dust receptor regions are shown as US-CARIB (red rectangle) and AMZN (green rectangle). The MERRA-2 mean annual dust emission values are projected and represented by the color bar. The brown rectangle is where the HYSPLIT forward trajectories are initiated following observed dust emission activities.

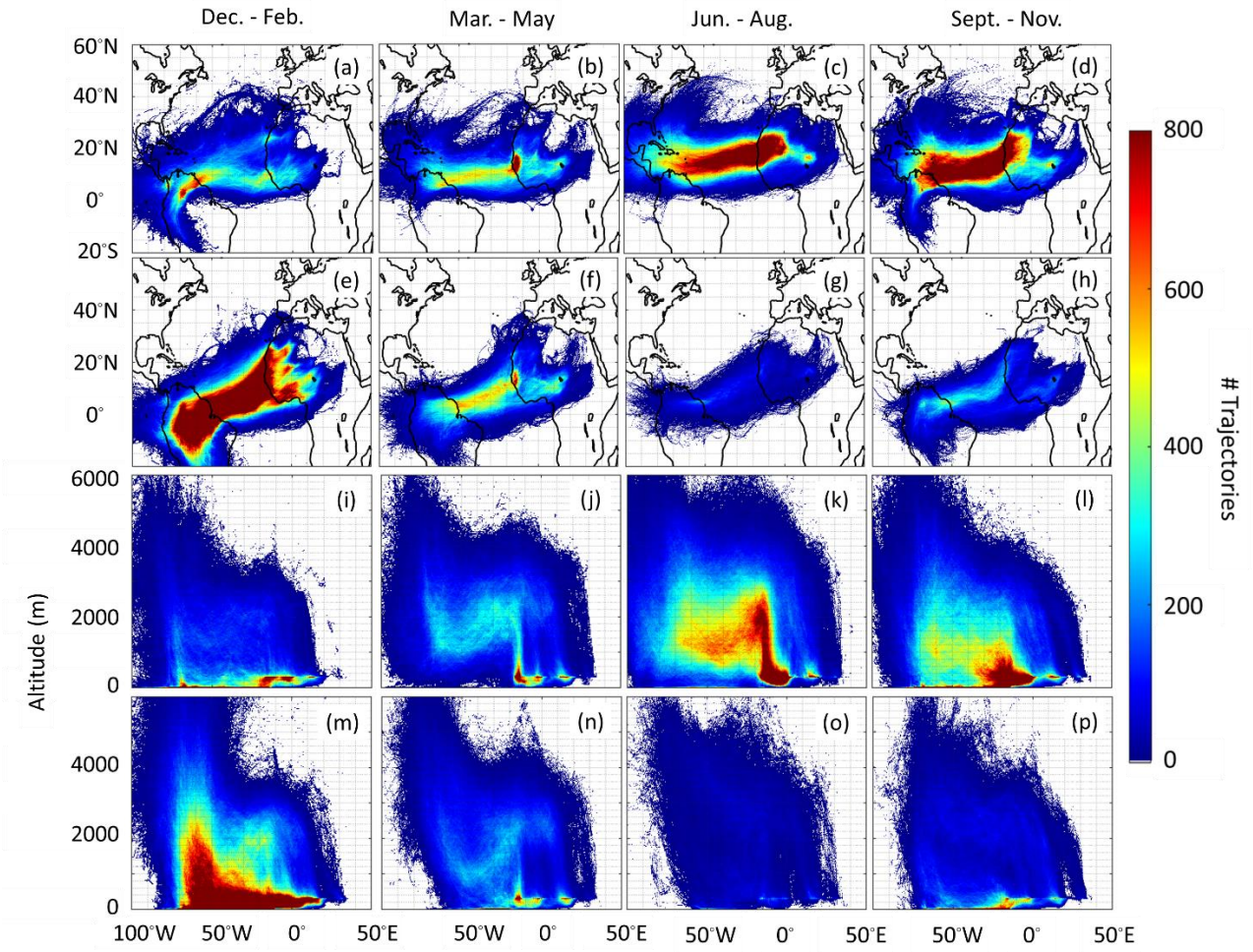

Figure 2. Seasonal trajectory density maps for US-CARIB (a - d) and AMZN (e - h) receptor regions during December – February, March – May, June – August, and September – November. Seasonal density maps of the altitudes taken by trajectories from the point of emission until reaching US-CARIB (i - l) and AMZN (m - p). Panels are made with 115,715 total number of trajectories impacting either one of receptor regions.

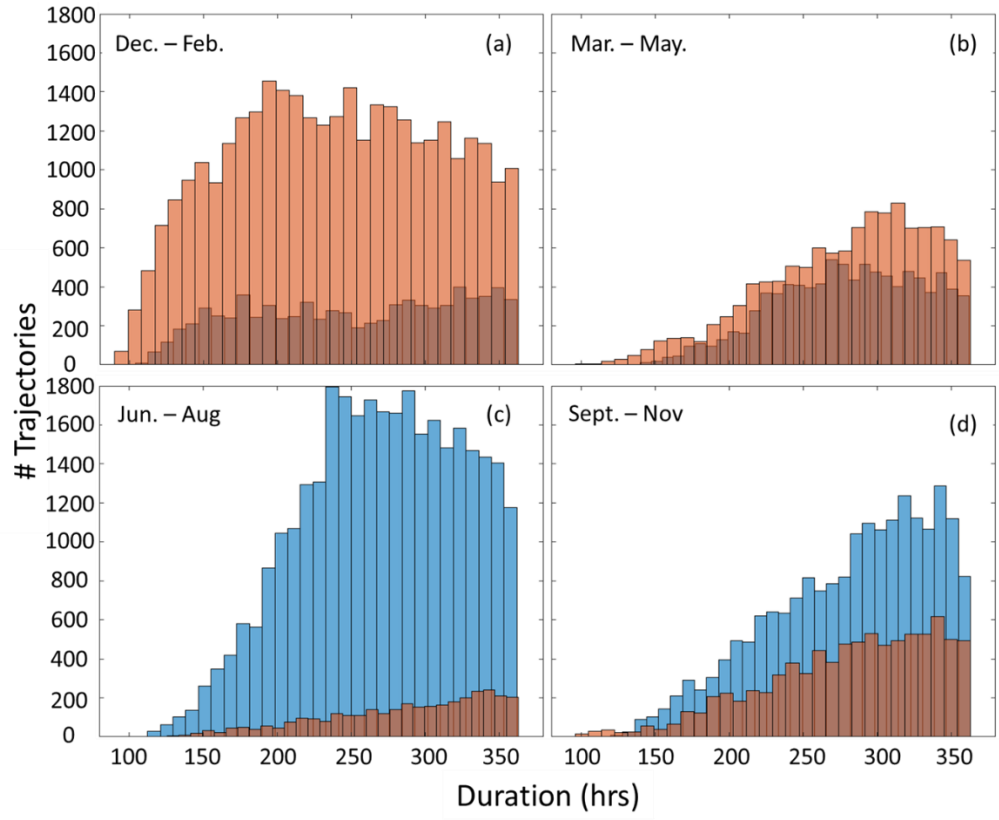

717

718 **Figure 3.** Seasonal histograms of travel duration for trajectories reaching the US-CARIB (blue),
719 and AMZN (orange) during December – February, March – May, June – August, and September
720 – November. Histograms are made with a total number of 124,677 trajectories, including 8,962
721 trajectories that are accounted for both sub-domains.

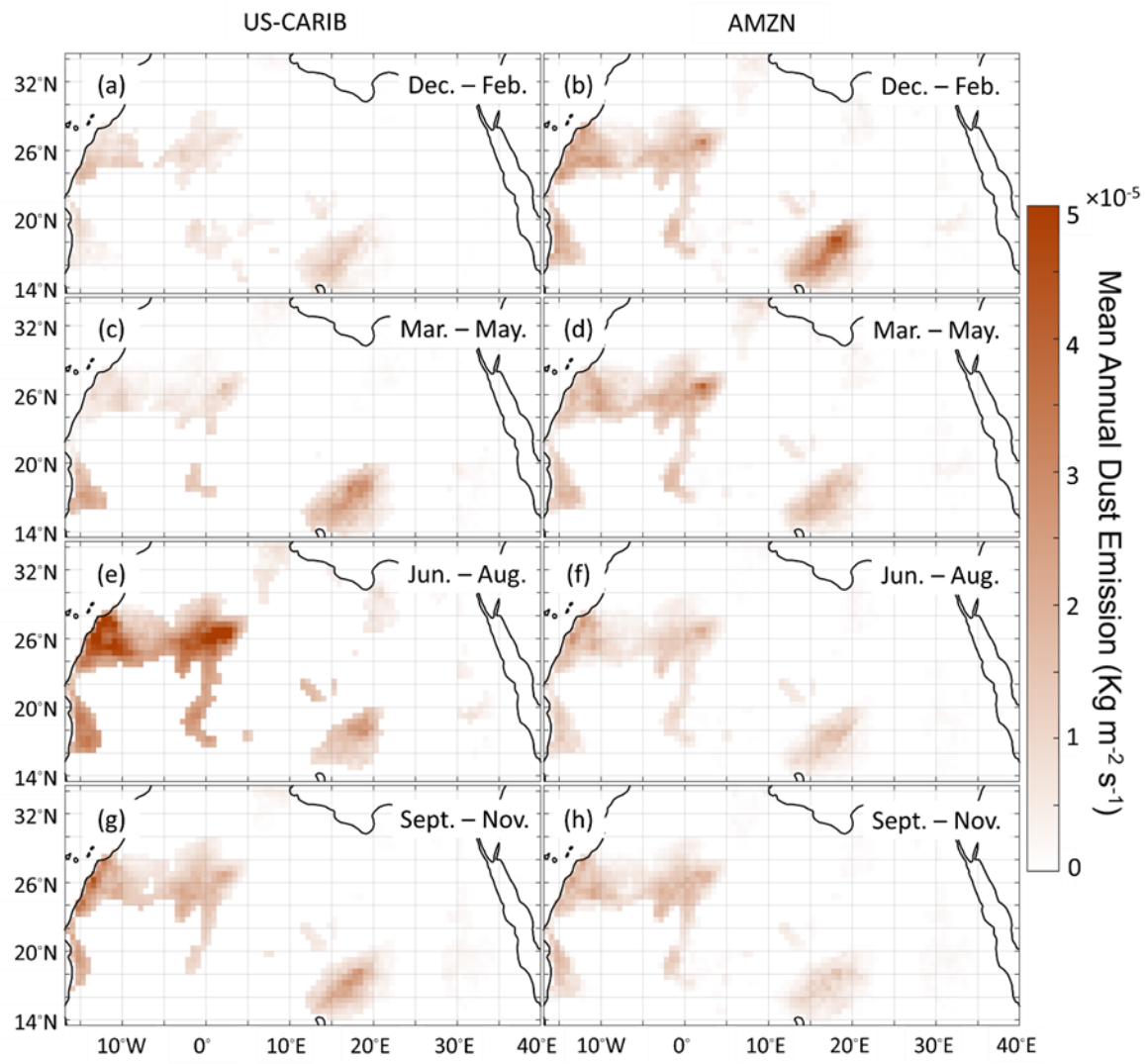

Figure 4. Total seasonal dust emissions associated with trajectories impacting US-CARIB (a, c, e, and g) and AMZN (b, d, f, and h) based on the NASA Modern-Era Retrospective analysis for Research and Applications, Version 2 (MERRA-2) dust emission dataset. Seasonal number of trajectories impacting each receptor sub-domain are summarized in Table 1, including 8962 trajectories accounted for both sub-domains.

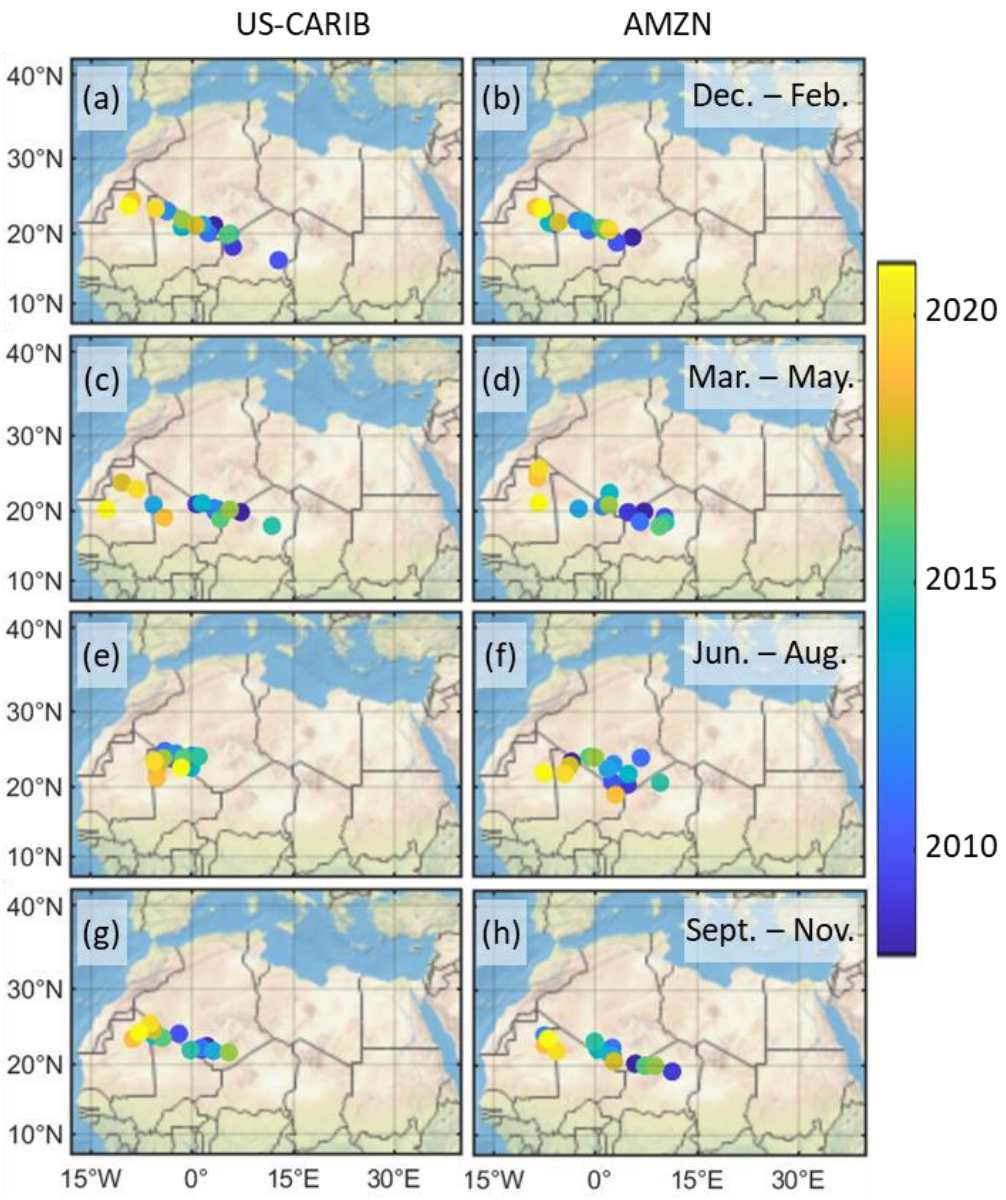

Figure 5. The seasonal location of the equivalent dust emission centers during December – February, March – May, June – August, and September – November, for trajectories impacting each receptor region. Panels a, c, e, and g belong to the US-CARIB and panels b, d, f, and h belong to AMZN region. Circles are color coded based on the year they belong to.

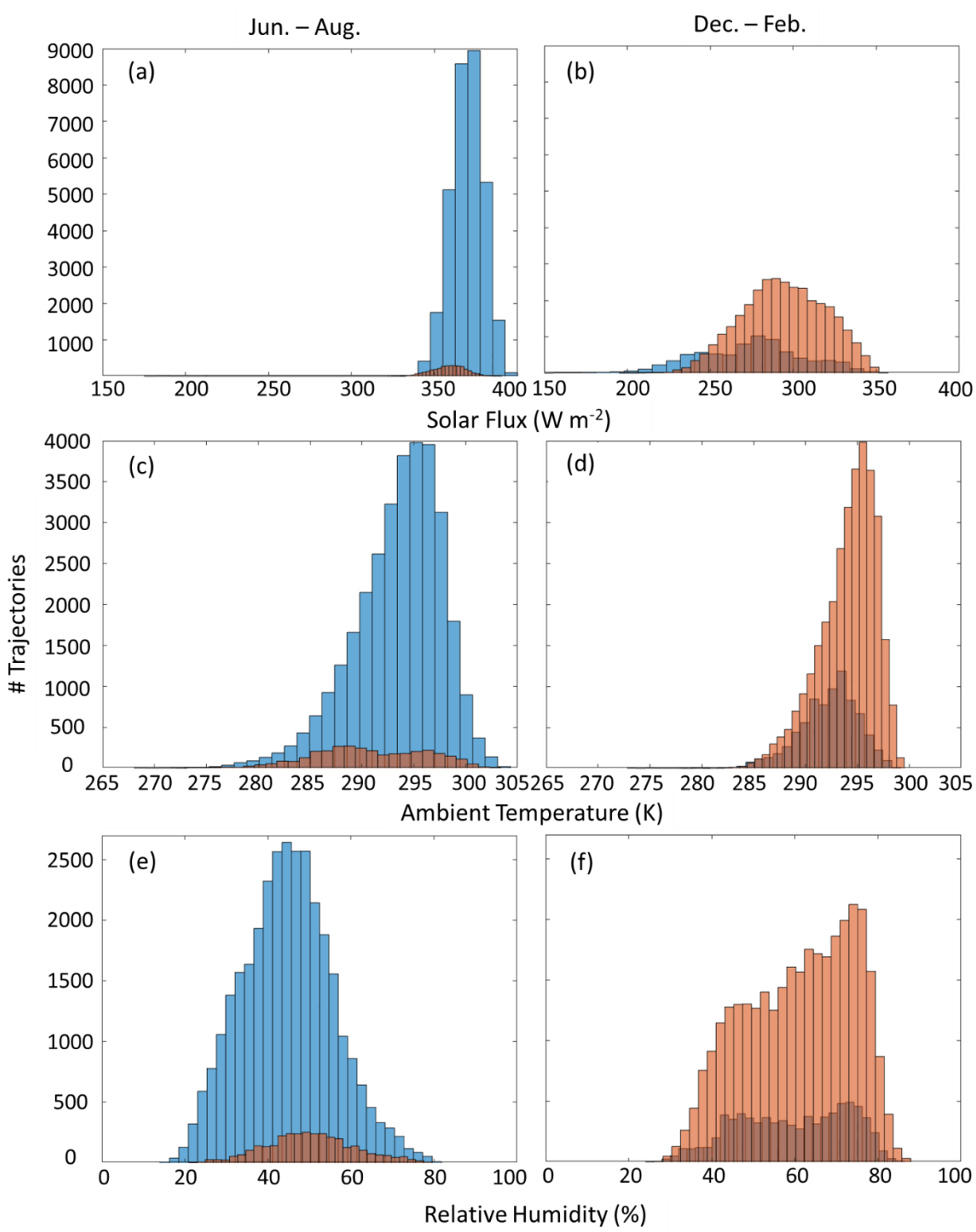

734

735 **Figure 6.** Histograms of average conditions along the trajectories impacting US-CARIB (Blue)
736 and AMZN (Orange) for solar radiation flux (a and b), ambient temperature (c and d), RH (e and
737 f). Only peak seasons of June - August for US-CARIB and December - February for AMZN are
738 compared.

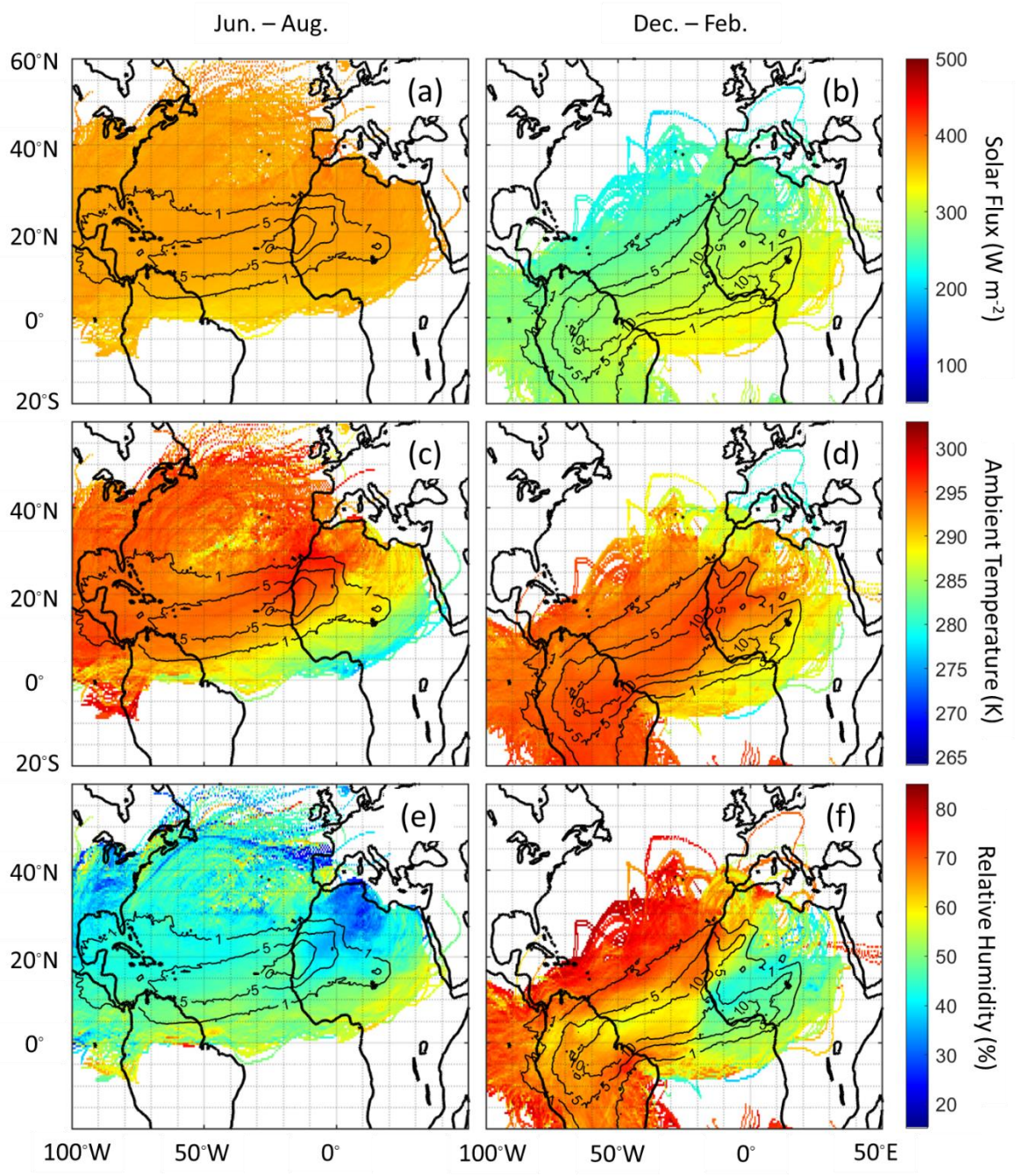

Figure 7. Average parameters along the trajectories impacting US-CARIB during the June - August season (a, c, and e) and AMZN during the December - February season (b, d, and f). Areas denoted by black contour lines represent pixels having at least 1, 5, and 10 percent of the total dust emission for trajectories passing above them, respectively.

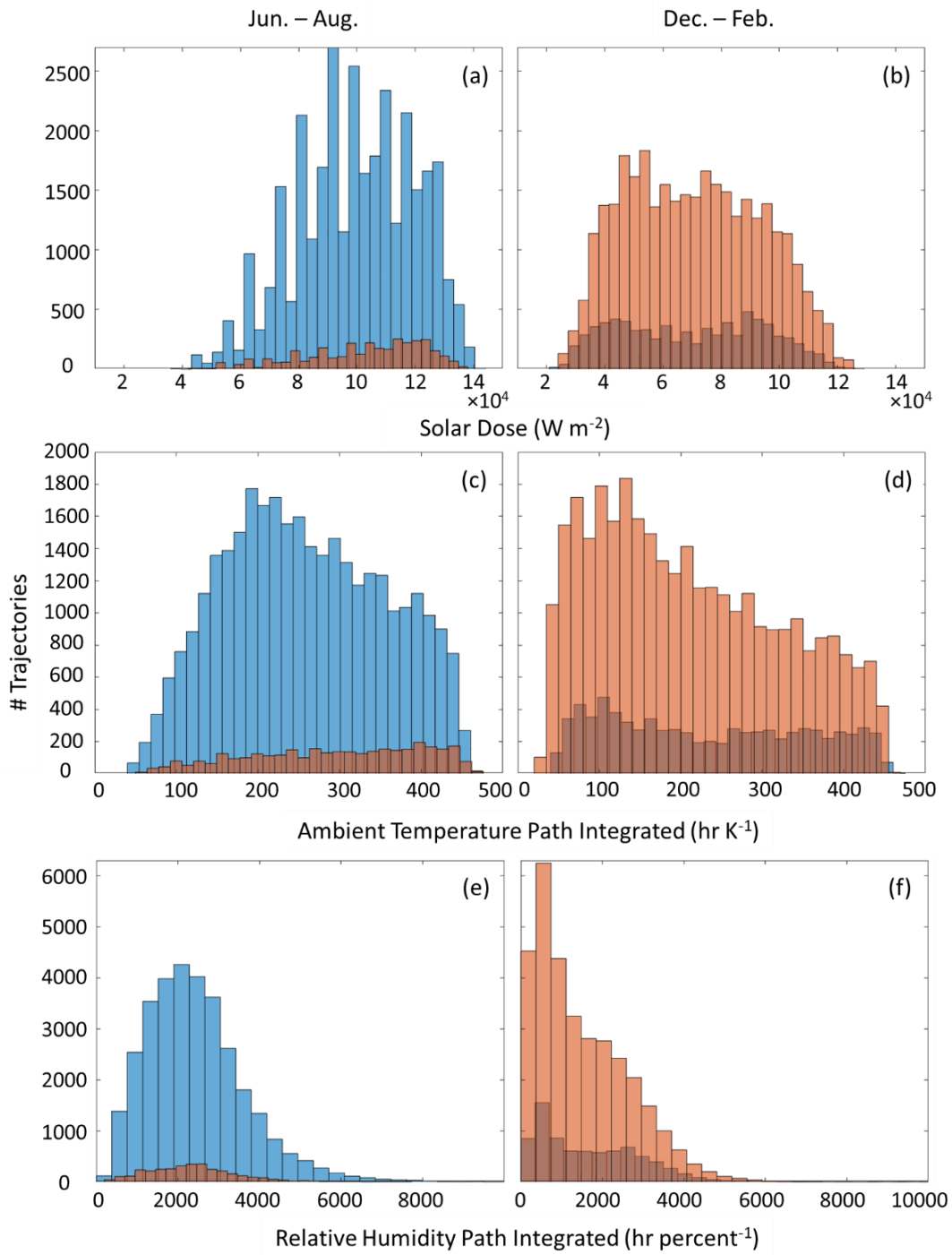

746

747 **Figure 8.** Histograms of path-integrated meteorological parameters along the trajectories
748 impacting US-CARIB (Blue) and AMZN (Orange) for solar dose flux (a and b), ambient
749 temperature (c and d), and RH (e and f). Only peak seasons of June - August for US-CARIB and
750 December - February for AMZN are compared. A higher path integrated value of temperature or
751 RH reflects a lower temperature or RH level impacting the aerosols for a longer period of time.

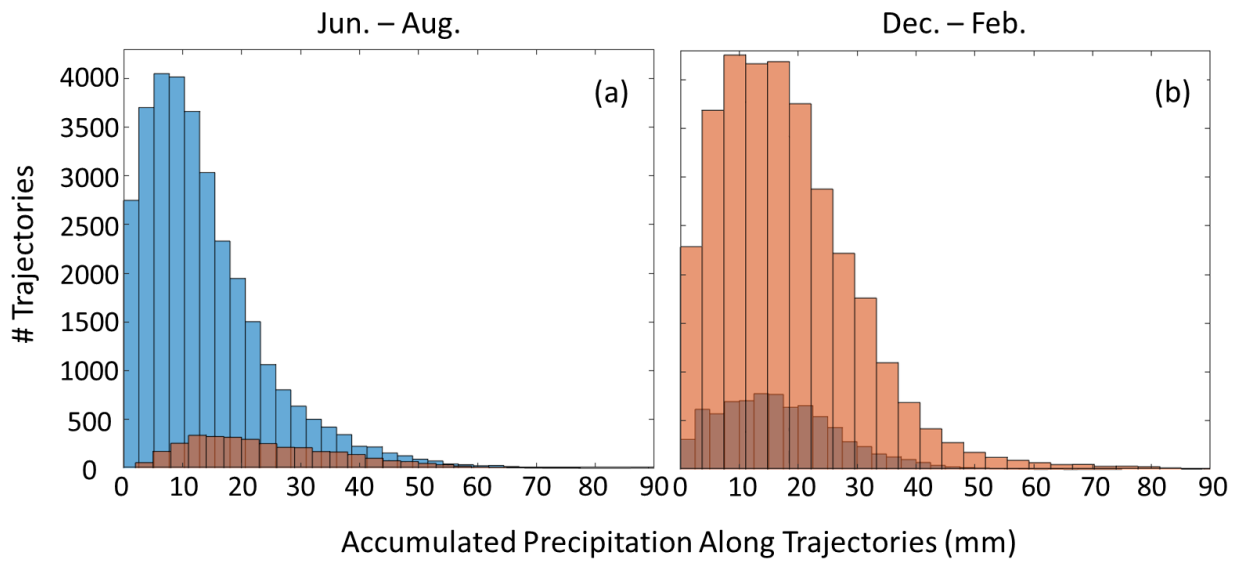

752
753
754 **Figure 9.** Histograms of accumulated precipitation along the trajectories for seasons of (a) June
755 – August and (b) December – February. Blue and orange denote trajectories impacting US-CARIB
756 and AMZN, respectively.
757
758
759
760

References

Almaguer, M., Aira, M. J., Rodríguez-Rajo, F. J., & Rojas, T. I. (2014). Temporal dynamics of airborne fungi in Havana (Cuba) during dry and rainy seasons: influence of meteorological parameters. International Journal of Biometeorology, 58(7), 1459-1470.

d'Almeida, G. A. (1986). A model for Saharan dust transport. Journal of Applied Meteorology and Climatology, 25(7), 903-916.

Arimoto, R., Duce, R. A., Ray, B. J., & Tomza, U. (2003). Dry deposition of trace elements to the western North Atlantic. Global biogeochemical cycles, 17(1).

Barkley, A. E., Pourmand, A., Longman, J., Sharifi, A., Prospero, J. M., Panechou, K., ... & Gaston, C. J. (2022). Interannual variability in the source location of North African dust transported to the Amazon. Geophysical Research Letters, e2021GL097344.

Barreiro, M., Chang, P., & Saravanan, R. (2002). Variability of the South Atlantic convergence zone simulated by an atmospheric general circulation model. Journal of Climate, 15(7), 745-763.

Bowers, R. M., McCubbin, I. B., Hallar, A. G., & Fierer, N. (2012). Seasonal variability in airborne bacterial communities at a high-elevation site. Atmospheric Environment, 50, 41-49.

Bristow, Charlie S., Karen A. Hudson-Edwards, and Adrian Chappell. "Fertilizing the Amazon and equatorial Atlantic with West African dust." Geophysical Research Letters 37.14 (2010).

Brooks, N., & Legrand, M. (2000). Dust variability over northern Africa and rainfall in the Sahel. Linking climate change to land surface change, 1-25.

Brown, J. K., & Hovmøller, M. S. (2002). Aerial dispersal of pathogens on the global and continental scales and its impact on plant disease. Science, 297(5581), 537-541.

Burrows, S. M., Butler, T., Jöckel, P., Tost, H., Kerkweg, A., Pöschl, U., & Lawrence, M. G. (2009). Bacteria in the global atmosphere–Part 2: Modeling of emissions and transport between different ecosystems. Atmospheric Chemistry and Physics, 9(23), 9281-9297.

Burrows, S. M., Elbert, W., Lawrence, M. G., & Pöschl, U. (2009). Bacteria in the global atmosphere–Part 1: Review and synthesis of literature data for different ecosystems. Atmospheric Chemistry and Physics, 9(23), 9263-9280.

Cáliz, J., Triadó-Margarit, X., Camarero, L., & Casamayor, E. O. (2018). A long-term survey unveils strong seasonal patterns in the airborne microbiome coupled to general and regional atmospheric circulations. Proceedings of the National Academy of Sciences, 115(48), 12229-12234.

Chakraborty, S., Guan, B., Waliser, D. E., da Silva, A. M., Uluatam, S., & Hess, P. (2021). Extending the Atmospheric River Concept to Aerosols: Climate and Air Quality Impacts. Geophysical Research Letters, 48(9), e2020GL091827.

Chen, X., Kumari, D., & Achal, V. (2020). A review on airborne microbes: the characteristics of sources, pathogenicity and geography. Atmosphere, 11(9), 919.

Chiapello, I., Moulin, C., & Prospero, J. M. (2005). Understanding the long-term variability of African dust transport across the Atlantic as recorded in both Barbados surface concentrations and large-scale Total Ozone Mapping Spectrometer (TOMS) optical thickness. Journal of Geophysical Research: Atmospheres, 110(D18).

Dadashazar, H., Alipanah, M., Hilario, M. R. A., Crosbie, E., Kirschler, S., Liu, H., ... & Sorooshian, A. (2021). Aerosol responses to precipitation along North American air trajectories arriving at Bermuda. Atmospheric chemistry and physics, 21(21), 16121-16141.

Doherty, O. M., Riemer, N., & Hameed, S. (2012). Control of Saharan mineral dust transport to Barbados in winter by the Intertropical Convergence Zone over West Africa. Journal of Geophysical Research: Atmospheres, 117(D19).

Draxler, R. R., & Rolph, G. D. (2010). HYSPLIT (HYbrid Single-Particle Lagrangian Integrated Trajectory) model access via NOAA ARL READY website (http://ready. arl. noaa. gov/HYSPLIT. php), NOAA Air Resources Laboratory. Silver Spring, MD, 25.

Dunion, J. P. (2011). Rewriting the climatology of the tropical North Atlantic and Caribbean Sea atmosphere. Journal of Climate, 24(3), 893-908.

Dunion, J. P., & Marron, C. S. (2008). A reexamination of the Jordan mean tropical sounding based on awareness of the Saharan air layer: Results from 2002. Journal of Climate, 21(20), 5242-5253.

Engelstaedter, S., Tegen, I., & Washington, R. (2006). North African dust emissions and transport. Earth-Science Reviews, 79(1-2), 73-100.

Favet, J., Lapanje, A., Giongo, A., Kennedy, S., Aung, Y. Y., Cattaneo, A., ... & Gorbushina, A. A. (2013). Microbial hitchhikers on intercontinental dust: catching a lift in Chad. The ISME journal, 7(4), 850-867.

Freitag, S., Clarke, A. D., Howell, S. G., Kapustin, V. N., Campos, T., Brekhovskikh, V. L., & Zhou, J. (2014). Combining airborne gas and aerosol measurements with HYSPLIT: a visualization tool for simultaneous evaluation of air mass history and back trajectory consistency. Atmospheric Measurement Techniques, 7(1), 107-128.

Gat, D., Mazar, Y., Cytryn, E., & Rudich, Y. (2017). Origin-dependent variations in the atmospheric microbiome community in Eastern Mediterranean dust storms. Environmental science & technology, 51(12), 6709-6718.

Ginoux, P., Prospero, J. M., Gill, T. E., Hsu, N. C., & Zhao, M. (2012). Global-scale attribution of anthropogenic and natural dust sources and their emission rates based on MODIS Deep Blue aerosol products. Reviews of Geophysics, 50(3).

Giongo, A., Favet, J., Lapanje, A., Gano, K. A., Kennedy, S., Davis-Richardson, A. G., ... & Triplett, E. W. (2013). Microbial hitchhikers on intercontinental dust: high-throughput sequencing to catalogue microbes in small sand samples. Aerobiologia, 29(1), 71-84.

Gelaro, R., McCarty, W., Suárez, M. J., Todling, R., Molod, A., Takacs, L., ... & Zhao, B. (2017). The modern-era retrospective analysis for research and applications, version 2 (MERRA-2). Journal of climate, 30(14), 5419-5454.

Gläser, G., Wernli, H., Kerkweg, A., & Teubler, F. (2015). The transatlantic dust transport from North Africa to the Americas—Its characteristics and source regions. Journal of Geophysical Research: Atmospheres, 120(21), 11-231.

González-Martín, C., Pérez-González, C. J., González-Toril, E., Expósito, F. J., Aguilera, Á., & Díaz, J. P. (2021). Airborne bacterial community composition according to their origin in Tenerife, Canary Islands. Frontiers in microbiology, 12.

Gonzalez-Martin, C., Teigell-Perez, N., Valladares, B., & Griffin, D. W. (2014). The global dispersion of pathogenic microorganisms by dust storms and its relevance to agriculture. Advances in agronomy, 127, 1-41.

Gorbushina, A. A., Kort, R., Schulte, A., Lazarus, D., Schnetger, B., Brumsack, H. J., ... & Favet, J. (2007). Life in Darwin's dust: intercontinental transport and survival of microbes in the nineteenth century. Environmental Microbiology, 9(12), 2911-2922.

Gregory, P. H. (1961). The microbiology of the atmosphere. The microbiology of the atmosphere.

Gregory, P. H. (1971). The Leeuwenhoek Lecture 1970 Airborne microbes: their significance and distribution. Proceedings of the Royal Society of London. Series B. Biological Sciences, 177(1049), 469-483.

Griffin, D. W. (2007). Atmospheric movement of microorganisms in clouds of desert dust and implications for human health. Clinical microbiology reviews, 20(3), 459-477.

Griffin, D. W., Garrison, V. H., Herman, J. R., & Shinn, E. A. (2001). African desert dust in the Caribbean atmosphere: microbiology and public health. Aerobiologia, 17(3), 203-213.

Griffin, D. W., Kellogg, C. A., & Shinn, E. A. (2001). Dust in the wind: long range transport of dust in the atmosphere and its implications for global public and ecosystem health. Global Change and Human Health, 2(1), 20-33.

Grini, A., Myhre, G., Zender, C. S., & Isaksen, I. S. (2005). Model simulations of dust sources and transport in the global atmosphere: Effects of soil erodibility and wind speed variability. Journal of Geophysical Research: Atmospheres, 110(D2).

Hara, K., & Zhang, D. (2012). Bacterial abundance and viability in long-range transported dust. Atmospheric Environment, 47, 20-25.

Harris, J. M., Draxler, R. R., & Oltmans, S. J. (2005). Trajectory model sensitivity to differences in input data and vertical transport method. Journal of Geophysical Research: Atmospheres, 110(D14).

Harrison, R. M., Jones, A. M., Biggins, P. D., Pomeroy, N., Cox, C. S., Kidd, S. P., ... & Beswick, A. (2005). Climate factors influencing bacterial count in background air samples. International Journal of Biometeorology, 49(3), 167-178.

Heinold, B., Knippertz, P., Marsham, J. H., Fiedler, S., Dixon, N. S., Schepanski, K., ... & Tegen, I. (2013). The role of deep convection and nocturnal low-level jets for dust emission in summertime West Africa: Estimates from convection-permitting simulations. Journal of Geophysical Research: Atmospheres, 118(10), 4385-4400.

Herman, J. R., Krotkov, N., Celarier, E., Larko, D., & Labow, G. (1999). Distribution of UV radiation at the Earth's surface from TOMS-measured UV-backscattered radiances. Journal of Geophysical Research: Atmospheres, 104(D10), 12059-12076.

Hilario, M. R. A., Crosbie, E., Shook, M., Reid, J. S., Cambaliza, M. O. L., Simpas, J. B. B., ... & Sorooshian, A. (2021). Measurement report: Long-range transport patterns into the tropical northwest Pacific during the CAMP 2 Ex aircraft campaign: chemical composition, size distributions, and the impact of convection. Atmospheric Chemistry and Physics, 21(5), 3777-3802.

Iwasaka, Y., Minoura, H., & Nagaya, K. (1983). The transport and spacial scale of Asian dust-storm clouds: a case study of the dust-storm event of April 1979. Tellus B: Chemical and Physical Meteorology, 35(3), 189-196.

Jaenicke, R. (2005). Abundance of cellular material and proteins in the atmosphere. Science, 308(5718), 73-73.

Kaaden, N., Massling, A., Schladitz, A., Müller, T., Kandler, K., Schütz, L., ... & Wiedensohler, A. (2009). State of mixing, shape factor, number size distribution, and hygroscopic growth of the Saharan anthropogenic and mineral dust aerosol at Tinfou, Morocco. Tellus B: Chemical and Physical Meteorology, 61(1), 51-63.

Karyampudi, V. M., & Carlson, T. N. (1988). Analysis and numerical simulations of the Saharan air layer and its effect on easterly wave disturbances. Journal of the Atmospheric Sciences, 45(21), 3102-3136.

Kellogg, C. A., & Griffin, D. W. (2006). Aerobiology and the global transport of desert dust. Trends in ecology & evolution, 21(11), 638-644.

Kinne, S., Schulz, M., Textor, C., Guibert, S., Balkanski, Y., Bauer, S. E., ... & Tie, X. (2006). An AeroCom initial assessment–optical properties in aerosol component modules of global models. Atmospheric Chemistry and Physics, 6(7), 1815-1834.

Koehler, K. A., Kreidenweis, S. M., DeMott, P. J., Petters, M. D., Prenni, A. J., & Carrico, C. M. (2009). Hygroscopicity and cloud droplet activation of mineral dust aerosol. Geophysical Research Letters, 36(8).

Kok, J. F., Adebiyi, A. A., Albani, S., Balkanski, Y., Checa-Garcia, R., Chin, M., ... & Whicker, C. A. (2021). Improved representation of the global dust cycle using observational constraints on dust properties and abundance. Atmospheric Chemistry and Physics, 21(10), 8127-8167.

Kok, J. F., Adebiyi, A. A., Albani, S., Balkanski, Y., Checa-Garcia, R., Chin, M., ... & Wan, J. S. (2021). Contribution of the world's main dust source regions to the global cycle of desert dust. Atmospheric Chemistry and Physics, 21(10), 8169-8193.

Kowalski, W. (2010). Ultraviolet germicidal irradiation handbook: UVGI for air and surface disinfection. Springer science & business media.

Kowalski, M., & Pastuszka, J. S. (2018). Effect of ambient air temperature and solar radiation on changes in bacterial and fungal aerosols concentration in the urban environment. Annals of Agricultural and Environmental Medicine, 25(2), 259-261.

Li, Y., Randerson, J. T., Mahowald, N. M., & Lawrence, P. J. (2021). Deforestation strengthens atmospheric transport of mineral dust and phosphorus from North Africa to the Amazon. Journal of Climate, 34(15), 6087-6096.

Maring, H., Savioe, D. L., Izaguirre, M. A., Custals, L., & Reid, J. S. (2003). Vertical distributions of dust and sea-salt aerosols over Puerto Rico during PRIDE measured from a light aircraft. Journal of Geophysical Research: Atmospheres, 108(D19).

Mayol, E., Arrieta, J. M., Jiménez, M. A., Martínez-Asensio, A., Garcias-Bonet, N., Dachs, J., ... & Duarte, C. M. (2017). Long-range transport of airborne microbes over the global tropical and subtropical ocean. Nature Communications, 8(1), 1-9.

Mazar, Y., Cytryn, E., Erel, Y., & Rudich, Y. (2016). Effect of dust storms on the atmospheric microbiome in the Eastern Mediterranean. Environmental science & technology, 50(8), 4194-4202.

Mouli, P., Mohan, S., & Reddy, S. (2005). Assessment of microbial(bacteria) Concentrations of ambient air at semi-arid urban region: Influence of meteorological factors. Applied ecology and environmental research, 3(2), 139-149.

Musilova, M., Wright, G., Ward, J. M., & Dartnell, L. R. (2015). Isolation of radiation-resistant bacteria from Mars analog Antarctic Dry Valleys by preselection, and the correlation between radiation and desiccation resistance. Astrobiology, 15(12), 1076-1090.

Núñez, A., García, A. M., Moreno, D. A., & Guantes, R. (2021). Seasonal changes dominate long-term variability of the urban air microbiome across space and time. Environment International, 150, 106423.

Prospero, J. M., Blades, E., Mathison, G., & Naidu, R. (2005). Interhemispheric transport of viable fungi and bacteria from Africa to the Caribbean with soil dust. Aerobiologia, 21(1), 1-19.

Prospero, J. M., Ginoux, P., Torres, O., Nicholson, S. E., & Gill, T. E. (2002). Environmental characterization of global sources of atmospheric soil dust identified with the Nimbus 7 Total Ozone Mapping Spectrometer (TOMS) absorbing aerosol product. Reviews of geophysics, 40(1), 2-1.

Prospero, J. M., Collard, F. X., Molinié, J., & Jeannot, A. (2014). Characterizing the annual cycle of African dust transport to the Caribbean Basin and South America and its impact on the environment and air quality. Global Biogeochemical Cycles, 28(7), 757-773.

Prospero, J. M. (1999). Long-term measurements of the transport of African mineral dust to the southeastern United States: Implications for regional air quality. Journal of Geophysical Research: Atmospheres, 104(D13), 15917-15927.

Qin, W., Fang, H., Wang, L., Wei, J., Zhang, M., Su, X., ... & Liang, X. (2021). MODIS high-resolution MAIAC aerosol product: Global validation and analysis. Atmospheric Environment, 264, 118684.

Rahav, E., Paytan, A., Chien, C. T., Ovadia, G., Katz, T., & Herut, B. (2016). The impact of atmospheric dry deposition associated microbes on the southeastern mediterranean sea surface water following an intense dust storm. Frontiers in Marine Science, 3, 127.

Rainey, F. A., Ray, K., Ferreira, M., Gatz, B. Z., Nobre, M. F., Bagaley, D., ... & da Costa, M. S. (2005). Extensive diversity of ionizing-radiation-resistant bacteria recovered from Sonoran Desert soil and description of nine new species of the genus Deinococcus obtained from a single soil sample. Applied and environmental microbiology, 71(9), 5225-5235.

Randles, C. A., Da Silva, A. M., Buchard, V., Colarco, P. R., Darmenov, A., Govindaraju, R., ... & Flynn, C. J. (2017). The MERRA-2 aerosol reanalysis, 1980 onward. Part I: System description and data assimilation evaluation. Journal of climate, 30(17), 6823-6850.

Rolph, G. D., Stein, A., & Stunder, B. (2017). Real-time environmental applications and display system: Ready. Environmental Modelling & Software, 95, 210–228.

Schepanski, K., Heinold, B., & Tegen, I. (2017). Harmattan, Saharan heat low, and West African monsoon circulation: modulations on the Saharan dust outflow towards the North Atlantic. Atmospheric Chemistry and Physics, 17(17), 10223-10243.

Schepanski, K., Tegen, I., & Macke, A. (2009). Saharan dust transport and deposition towards the tropical northern Atlantic. Atmospheric Chemistry and Physics, 9(4), 1173-1189.

Schlesinger, P., Mamane, Y., & Grishkan, I. (2006). Transport of microorganisms to Israel during Saharan dust events. Aerobiologia, 22(4), 259-273.

Schuerger, A. C., Smith, D. J., Griffin, D. W., Jaffe, D. A., Wawrik, B., Burrows, S. M., ... & Yu, H. (2018). Science questions and knowledge gaps to study microbial transport and survival in Asian and African dust plumes reaching North America. Aerobiologia, 34(4), 425-435.

Schütz, L. (1980). Long range transport of desert dust with special emphasis on the Sahara. Annals of the New York Academy of Sciences, 338(1), 515-532.

Sengupta, S., Sengupta, S., Chanda, C. K., & Saha, H. (2021). Modeling the effect of relative humidity and precipitation on photovoltaic dust accumulation processes. IEEE Journal of Photovoltaics, 11(4), 1069-1077.

Shao, Y. (Ed.). (2008). Physics and modelling of wind erosion. Dordrecht: Springer Netherlands.

Shi, Y., Lai, S., Liu, Y., Gromov, S., & Zhang, Y. (2022). Fungal aerosol diversity over the northern South China Sea: the influence of land and ocean. Journal of Geophysical Research: Atmospheres, 127(6), e2021JD035213.

Shin, S. K., Kim, J., Ha, S. M., Oh, H. S., Chun, J., Sohn, J., & Yi, H. (2015). Metagenomic insights into the bioaerosols in the indoor and outdoor environments of childcare facilities. *PLoS One*, *10*(5), e0126960.

Shinn, E. A., Griffin, D. W., & Seba, D. B. (2003). Atmospheric transport of mold spores in clouds of desert dust. Archives of Environmental & Occupational Health, 58(8), 498.

Siongco, A. C., Hohenegger, C., & Stevens, B. (2017). Sensitivity of the summertime tropical Atlantic precipitation distribution to convective parameterization and model resolution in ECHAM6. Journal of Geophysical Research: Atmospheres, 122(5), 2579-2594.

Smith, D. J., Griffin, D. W., McPeters, R. D., Ward, P. D., & Schuerger, A. C. (2011). Microbial survival in the stratosphere and implications for global dispersal. Aerobiologia, 27(4), 319-332.

Stein, A. F., Draxler, R. R., Rolph, G. D., Stunder, B. J., Cohen, M. D., & Ngan, F. (2015). NOAA's HYSPLIT atmospheric transport and dispersion modeling system. Bulletin of the American Meteorological Society, 96(12), 2059-2077.

Sun, Y., Huang, Y., Xu, S., Li, J., Yin, M., & Tian, H. (2022). Seasonal variations in the characteristics of microbial community structure and diversity in atmospheric particulate matter from clean days and smoggy days in Beijing. Microbial ecology, 83(3), 568-582.

Tang, J. W. (2009). The effect of environmental parameters on the survival of airborne infectious agents. Journal of the Royal Society Interface, 6(suppl_6), S737-S746.

Tsamalis, C., Chédin, A., Pelon, J., & Capelle, V. (2013). The seasonal vertical distribution of the Saharan Air Layer and its modulation by the wind. Atmospheric Chemistry and Physics, 13(22), 11235-11257.

Uno, I., Eguchi, K., Yumimoto, K., Takemura, T., Shimizu, A., Uematsu, M., ... & Sugimoto, N. (2009). Asian dust transported one full circuit around the globe. Nature Geoscience, 2(8), 557-560.

Utrillas, M. P., Marín, M. J., Esteve, A. R., Salazar, G., Suárez, H., Gandía, S., & Martínez-Lozano, J. A. (2018). Relationship between erythemal UV and broadband solar irradiation at high altitude in Northwestern Argentina. Energy, 162, 136-147.

Van Der Does, M., Knippertz, P., Zschenderlein, P., Giles Harrison, R., & Stuut, J. B. W. (2018). The mysterious long-range transport of giant mineral dust particles. Science advances, 4(12), eaau2768.

Wagner, R., Schepanski, K., Heinold, B., & Tegen, I. (2016). Interannual variability in the Saharan dust source activation—Toward understanding the differences between 2007 and 2008. Journal of Geophysical Research: Atmospheres, 121(9), 4538-4562.

Washington, R., Bouet, C., Cautenet, G., Mackenzie, E., Ashpole, I., Engelstaedter, S., ... & Tegen, I. (2009). Dust as a tipping element: the Bodélé Depression, Chad. Proceedings of the National Academy of Sciences, 106(49), 20564-20571.

Washington, R., Todd, M., Middleton, N. J., & Goudie, A. S. (2003). Dust-storm source areas determined by the total ozone monitoring spectrometer and surface observations. Annals of the Association of American Geographers, 93(2), 297-313.

Williams, R. M. (1982). A model for the dry deposition of particles to natural water surfaces. Atmospheric Environment (1967), 16(8), 1933-1938.

Wotawa, G., & Kalinowski, M. B. (2000, December). Evaluation of the operational IDC ATM products by comparing HYSPLIT BA, FA and OMEGA FOR during Level 4 events in Scandinavia. In Proceedings of the Informal Workshop on Meteorological Modelling in Support of CTBT Verification (pp. 4-6).

Wulfmeyer, V., & Feingold, G. (2000). On the relationship between relative humidity and particle backscattering coefficient in the marine boundary layer determined with differential absorption lidar. Journal of Geophysical Research: Atmospheres, 105(D4), 4729-4741.

Yamaguchi, N., Ichijo, T., Sakotani, A., Baba, T., & Nasu, M. (2012). Global dispersion of bacterial cells on Asian dust. Scientific Reports, 2(1), 1-6.

Yang, Y., Itahashi, S., Yokobori, S. I., & Yamagishi, A. (2008). UV-resistant bacteria isolated from upper troposphere and lower stratosphere. Biological Sciences in Space, 22(1), 18-25.

Yu, H., Tan, Q., Zhou, L., Zhou, Y., Bian, H., Chin, M., ... & Holben, B. N. (2021). Observation and modeling of the historic “Godzilla” African dust intrusion into the Caribbean Basin and the southern US in June 2020. Atmospheric Chemistry and Physics, 21(16), 12359-12383.

Zhai, Y., Li, X., Wang, T., Wang, B., Li, C., & Zeng, G. (2018). A review on airborne microorganisms in particulate matters: composition, characteristics and influence factors. Environment international, 113, 74-90.

Zhang, S., Hou, S., Ma, X., Qin, D., & Chen, T. (2007). Culturable bacteria in Himalayan glacial ice in response to atmospheric circulation. Biogeosciences, 4(1), 1-9.

Zhen, Q., Deng, Y., Wang, Y., Wang, X., Zhang, H., Sun, X., & Ouyang, Z. (2017). Meteorological factors had more impact on airborne bacterial communities than air pollutants. Science of the Total Environment, 601, 703-712.